ACS OMEGA

http://pubs.acs.org/journal/acsodf

Article

# Interactions of the C-Terminal Truncated DEAD-Box Protein DDX3X With RNA and Nucleotide Substrates

Anthony F. T. Moore, Aliana López de Victoria, and Eda Koculi*

Cite This: *ACS Omega* 2021, 6, 12640−12646

Read Online

ACCESS | Metrics & More | Article Recommendations | Supporting Information

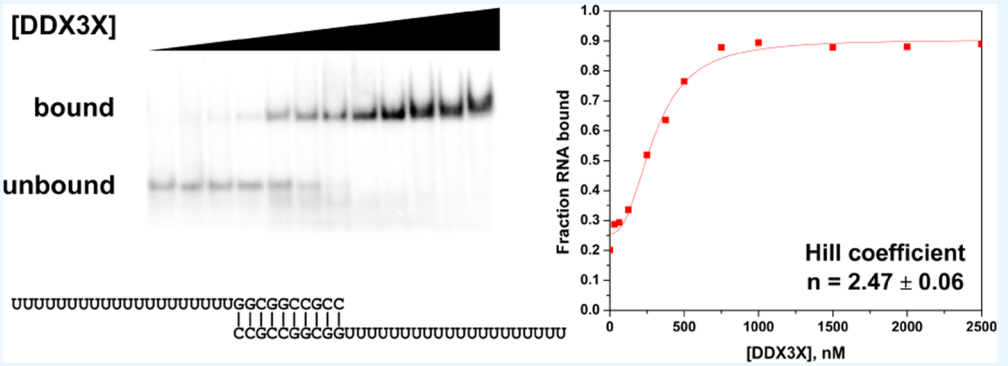


**ABSTRACT:** DDX3X is a human DEAD-box RNA helicase implicated in many important cellular processes. In addition to the RecA-like catalytic core, DDX3X contains N- and C-terminal domains. The ancillary domains of DEAD-box RNA helicases have been shown to modulate their interactions with RNA and nucleotide substrates. Here, with the goal of understanding the role of N- and C-terminal domains of DDX3X on the DDX3X catalytic activity, we examined the interactions of RNA substrates and nucleotides with a DDX3X construct possessing the entire N-terminal domain and the catalytic core but lacking 80 residues from its C-terminal domain. Next, we compared our results with previously investigated DDX3X constructs. Our data show that the C-terminal truncated DDX3X does not bind to a blunt-ended double-helix RNA. This conclusion agrees with the data obtained on the wild-type LAF-1 protein, the DDX3X ortholog in *Caenorhabditis elegans*, and disagrees with the data obtained on the minimally active DDX3X construct, which misses 131 residues from its N-terminal domain and 80 residues from its C-terminal domain. The minimally active DDX3X construct was able to bind to the blunt-ended RNA construct. Combined, the previous studies and our results indicate that the N-terminal of DDX3X modulates the choice of DDX3X−RNA substrates. Furthermore, a previous study showed that the wild-type DDX3X construct hydrolyzes all four nucleotides and deoxynucleotides, both in the presence and absence of RNA. The C-terminal truncated DDX3X investigated here hydrolyzes only cytidine triphosphate (CTP) in the absence of RNA and CTP, adenosine triphosphate (ATP), and deoxyribose adenosine triphosphate (dATP) in the presence of RNA. Hence, the C-terminal truncated DDX3X has a more stringent nucleotide specificity than wild-type DDX3X.

## INTRODUCTION

DEAD-box RNA helicases are a family of proteins implicated in all aspects of RNA metabolism.[1−3] This family of proteins contains two RecA-like domains that form the catalytic core.[1−4] For many DEAD-box RNA helicases, the catalytic core uses the energy of adenosine triphosphate (ATP) binding and hydrolysis to unwind short RNA double helixes in a sequence nonspecific manner.[2,3] DDX3X is a human DEAD-box RNA helicase that is involved in RNA transport, storage, splicing, translation, ribosome assembly and consequently is implicated in many human diseases.[3,5−8] The in vivo substrates of DEAD-box proteins remains largely uncharacterized.[3] Based on their in vitro RNA unwinding activity, many DEAD-box proteins are believed to serve as RNA chaperones.[9−12] The investigations of how the catalytic activity of DDX3X is regulated is important both for the understanding of its precise role in important cellular processes and for the design and development of potential therapeutic agents that target the DDX3X protein.

In addition to the catalytic core, DDX3X has N- and C-terminal domains.[13−15] The catalytic core of DDX3X is not sufficient for its catalytic activity, and fragments from N- and C-terminal domains are required for activity.[13−15] The minimally catalytically active DDX3X construct contains the

Received: February 7, 2021
Accepted: April 20, 2021
Published: May 6, 2021

Table 1. Sequences of RNA Molecules Used in This Study

| RNA molecules | sequences |
|---|---|
| A[a] | 5′-GGCGGCCGCC |
| B[b] | 5′-UUUUUUUUUUUUUUUUUUUUGGCGGCCGCC |
| C[c] | 5′-UUUUUUUUUUUUUUUUUUUUGGUGGUUGUG-3′ |
| D[d] | 5′-CUCAACUCAACCCUUCAUCUCAACUCAACCCUUCAU |
| E[d] | 5′-AUGAAGGGUUGAGUUGAGAUGAAGGGUUGAGUUGAG |

[a]The sequence of the RNA molecule A is palindromic. Two A molecules form a double helix with no overhangs. [b]The 3′-end of molecule B is palindromic. Two B molecules form a double helix with two 5′-end single-stranded overhangs. [c]The sequences of molecules B and C are similar. Five bases were changed in molecule B, out of 30, to create molecule C. The C molecule is unable to form a double helix by itself. [d]Molecule E is the reverse complementary of molecule D. The D:E molecule forms a double helix with no overhangs.

N-terminal residues 132−182, the catalytic core residues 183−544, and C-terminal residues 545−582.[14] Thus, this construct lacks the first 131 residues of the N-terminal domain and the last 80 residues of the C-terminal domain. The minimally active DDX3X construct binds to a blunt-ended double helix with a low affinity ($K_d \sim 10\ \mu M$).[14] However, this helix does not support the ATPase activity of the minimally active DDX3X construct, suggesting that the weak interaction between the blunt-ended, double-helix substrate and the separated DDX3X catalytic core does not produce the structural changes required to support ATP hydrolysis.[14,16] Interestingly, the wild-type LAF-1, DDX3X ortholog in *Caenorhabditis elegans*, containing both the N- and C-terminal domains, was unable to bind to a blunt-ended double helix.[17] Taken together, the experiments performed with the minimally active DDX3X construct[14] and the wild-type LAF-1 protein[17] suggest that the N- or C-terminal residues missing in the minimally active DDX3X construct but present in the wild-type LAF-1 protein could prevent the wild-type DDX3X from associating with blunt-ended, double-helix substrates, which are unable to support DDX3X's ATPase hydrolysis and likely its unwinding activity. To investigate this hypothesis, we probed the interaction of different RNA substrates with a DDX3X construct containing the complete N-terminal domain (residues 1−182), the catalytic core (residues 183−544), but having a truncated C-terminal domain. The C-terminal domain of the DDX3X construct investigated here contains residues 545−582 but lacks residues 583−662.

While the majority of DEAD-box proteins studied to date are unable to bind and hydrolyze other nucleotides besides ATP and deoxyribose adenosine triphosphate (dATP),[3,18] Mss166, a DEAD-box protein from *Saccharomyces cerevisiae* (*S.cerevisiae*), was shown to bind all four NTPs,[19] and DDX3X was shown to both bind and hydrolyze all four NTPs and dNTPs in the presence and absence of RNA substrates.[20,21] Here, we also investigated if the DDX3X C-terminal domain modulates its nucleotide substrate specificity.

## RESULTS

**Blunt-Ended RNA Double Helix does Not Support the ATPase Activity of the C-Terminal Truncated DDX3X.** The ATPase activity of the minimally active DDX3X construct was supported by substrate B:B, which contained single-stranded and double-stranded junctions, but not by substrate A:A, which consisted only of a double helix (Table 1).[14] Here, we investigated the ability of A:A and B:B substrates to stimulate the ATPase activity of the C-terminal truncated DDX3X using the malachite green/molybdate colorimetric assay.[22] The ATPase activity of the C-terminal truncated DDX3X is stimulated by substrate B:B but not A:A (Figure 1).

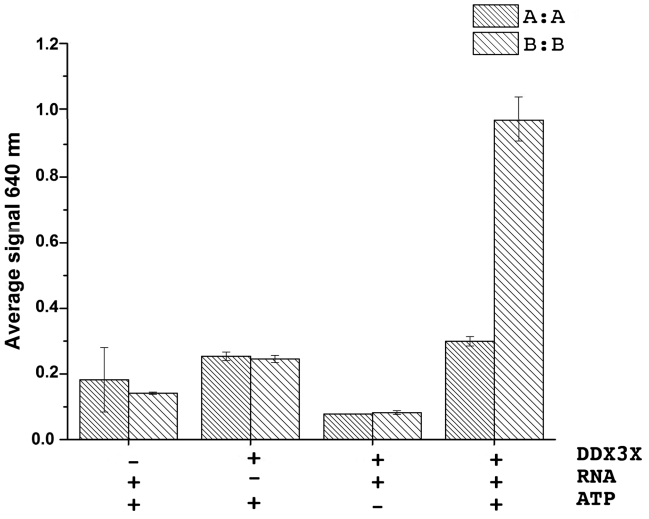


**Figure 1.** The RNA construct with single-stranded overhangs (B:B) supports the ATPase activity of DDX3X, while the blunt-ended RNA construct (A:A) does not. The ATP hydrolysis activity of DDX3X was measured by the malachite green assay, as described in the Methods section. The data shown are the averages of three independent experiments, and the errors are the standard deviations from the means.

Hence, similar to the minimally active DDX3X, the blunt-ended RNA double helix does not support the ATPase activity of the C-terminal truncated DDX3X, while the RNA construct containing single-stranded and double-stranded regions supports the C-terminal truncated DDX3X's ATPase activity.

**C-Terminal Truncated DDX3X does Not Bind to the Double-Stranded RNA Molecule.** To determine why the B:B substrate supported the ATPase activity of DDX3X while A:A did not, we performed electrophoretic mobility shift assays (EMSA). Figure 2A shows the dependence of the fraction RNA shifted versus the DDX3X protein concentration for substrates A:A, B:B, C, and D:E. Substrate B:B, which supports the ATPase activity of the C-terminal truncated DDX3X, also supports its binding. Example gels are shown in the Supporting Information (Figure S2). Using the Hill equation to fit the binding data of the C-terminal truncated DDX3X to substrate B:B, we obtained a Hill coefficient of 2.47 ± 0.06 (Table 2). Hence, the binding of the C-terminal truncated DDX3X to this substrate is a cooperative process.

A Hill coefficient of greater than one demonstrates that more than one protomer is bound cooperatively to the RNA substrate B:B.[23]

The single-stranded RNA substrate C also supports the binding of the C-terminal truncated DDX3X. However, the maximum fraction of the shifted RNA-C-terminal truncated


https://doi.org/10.1021/acsomega.1c00700
ACS Omega 2021, 6, 12640−12646

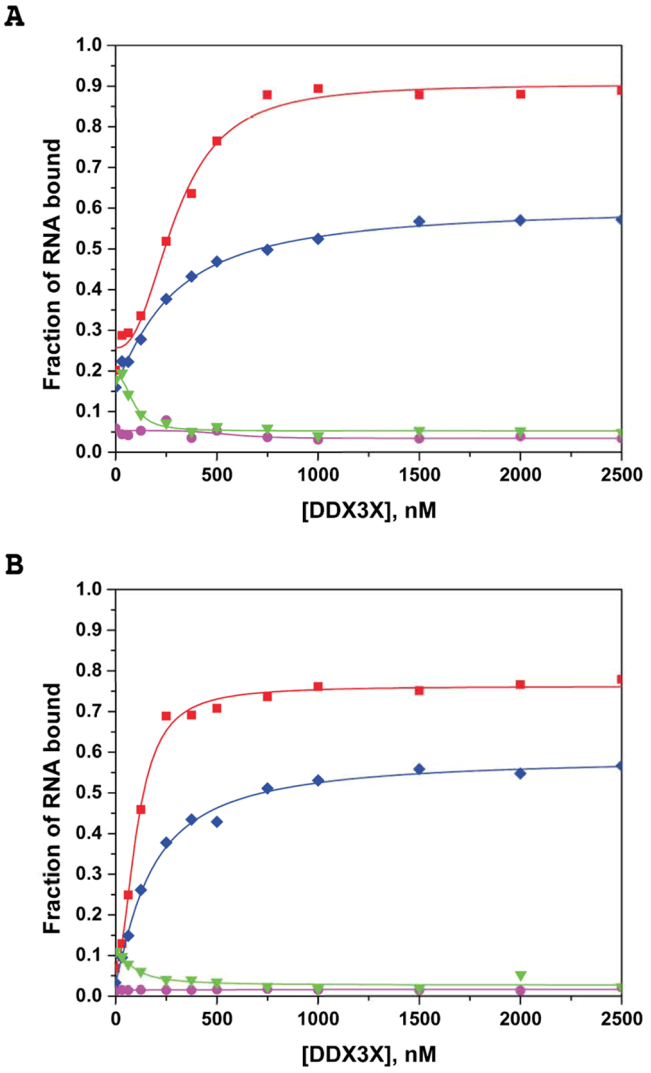


**Figure 2.** Equilibrium binding of DDX3X to various RNA substrates. (A) Representative plots of DDX3X binding to different RNA substrates in the absence of nucleotides; (B) representative plots of DDX3X binding to RNA in the presence of AMPPNP. Legend: substrate A:A (—circle—); substrate B:B (—square—); substrate C (—diamond—); and substrate D:E (—down-triangle—). Substrates' sequences are shown in Table 1. The average values for the Hill coefficient, dissociation constant, and their standard deviations are shown in Table 2.

DDX3X complex is smaller in the presence of substrate C instead of substrate B:B (Table 1 and Figure 2A). There are two possible explanations for these results. First, a fraction of substrate C is refractory to DDX3X binding. We investigated the structure of substrate C using RNA folding web application Mfold.[24] As predicted from Mfold, construct C does not form stable secondary structures. Therefore, all of the C molecules should support C-terminal truncated DDX3X binding in the same way. Another possibility is that substrate C in complex with the C-terminal truncated DDX3X is less stable than the substrate B:B in complex with the C-terminal truncated DDX3X, and a fraction of substrate C in complex with the protein is coming apart during electrophoresis.[25,26]

RNA substrate A:A (Table 1), which consists of only a double helix, does not support C-terminal truncated DDX3X binding, as investigated by EMSA. Consequently, the inability of the A:A substrate to support the ATPase activity of the C-terminal truncated DDX3X is a result of the A:A substrate's inability to support the C-terminal truncated DDX3X binding. Furthermore, we investigated the ability of a longer blunt-ended RNA substrate, D:E (Table 1), to support the C-terminal truncated DDX3X binding. This longer double-stranded construct is also unable to support DDX3X binding, demonstrating that the C-terminal truncated DDX3X does not bind to either short or long blunt-ended RNA double helices (Figure 2A).

**Table 2. Equilibrium Parameters of C-Terminal Truncated DDX3X–RNA Substrates' Interactions**

| | | DDX3X–RNA binding | |
|---|---|---|---|
| | | nucleotide | |
| RNA substrate | parameter[a] | –AMPPNP | +AMPPNP |
| A:A | $n$ | | |
| | $K_d$ (DDX3X, nM) | | |
| B:B | $n$ | 2.47 ± 0.06 | 2.06 ± 0.08 |
| | $K_d$ (DDX3X, nM) | 285 ± 18 | 114 ± 10 |
| C | $n$ | 1.30 ± 0.10 | 1.17 ± 0.01 |
| | $K_d$ (DDX3X, nM) | 298 ± 31 | 217 ± 60 |
| D:E | $n$ | | |
| | $K_d$ (DDX3X, nM) | | |

[a] $n$ and $K_d$ are the Hill coefficient and the dissociation constant, respectively. They were determined by fitting the Hill equation to the EMSA data. The values shown are the averages obtained by a minimum of two independent experiments, and the errors are the standard deviations from those averages.

Next, we investigated the effect of the nonhydrolyzable ATP analogue, AMPPNP, on the equilibrium binding of C-terminal truncated DDX3X to different RNA substrates. Figure 2B shows the fraction of RNA bound to C-terminal DDX3X versus protein concentrations in the presence of 6 mM AMPPNP. Example gels are shown in the Supporting Information (Figure S2).

The double-stranded RNA substrates A:A and D:E, which did not support C-terminal truncated DDX3X binding in the absence of AMPPNP, did not support the C-terminal truncated DDX3X binding when AMPPNP was present either. Substrate C supported the C-terminal truncated DDX3X binding with the same affinity and cooperativity in the presence or absence of AMPPNP. Substrate B:B supported the binding of the C-terminal truncated DDX3X with a higher affinity in the presence compared to the absence of AMPPNP (Table 2). The increased affinity of DEAD-box RNA helicases in the presence of AMPPNP has been observed for other DEAD-box proteins. For these DEAD-box proteins, the AMPPNP promotes the closed conformation of the RecA-like catalytic core, which increases the catalytic core's affinity for the RNA substrates.[27−36] Thus, our data indicate that constructs C and B:B interact differently with the C-terminal truncated DDX3X. Only the B:B substrate, which contains both single-stranded and double-stranded regions, supports the closed conformation of the catalytic core in the presence of AMPPNP. Finally, our results are similar to those obtained with Ded1p, the DDX3X ortholog in *S. cerevisiae*. Ded1p also shows an increase in the affinity in the presence of AMPPNP for an RNA construct containing single-stranded and double-stranded regions but not for a single-stranded RNA construct.[37]

**C-Terminal Truncated DDX3X Nucleotide Hydrolysis Preference.** The goal of these experiments is to investigate if


https://doi.org/10.1021/acsomega.1c00700
ACS Omega 2021, 6, 12640−12646

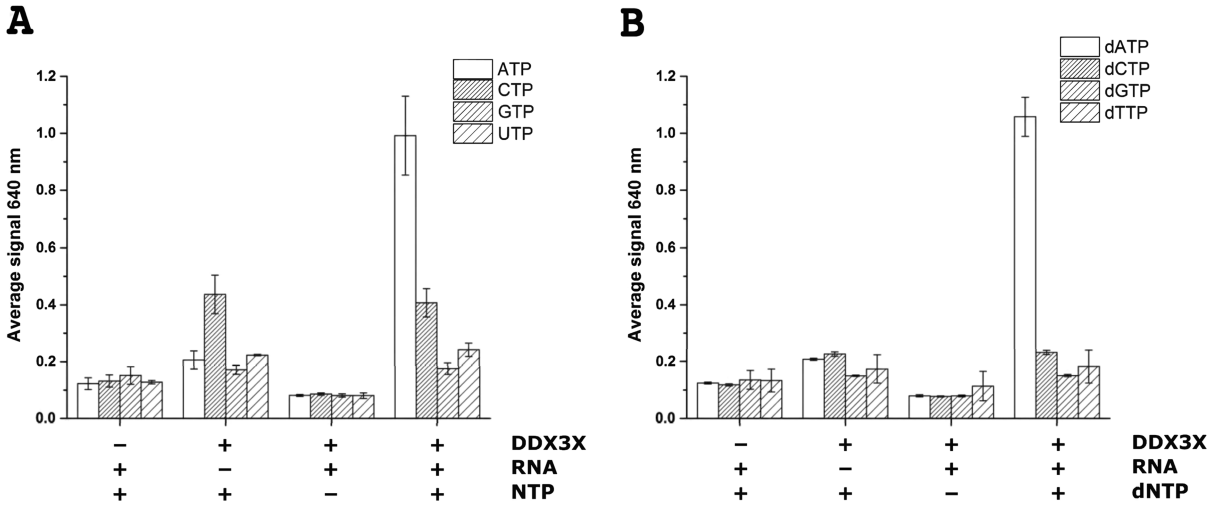


**Figure 3.** (A) DDX3X hydrolysis activity in the presence of various NTPs. (B) DDX3X hydrolysis activity in the presence of dNTPs. The hydrolysis activity of DDX3X was measured by the malachite green assay, as described in the Methods section. The data shown are the averages of three independent experiments and the errors are the standard deviations from the means. The RNA substrate used for these experiments was the B:B molecule (Table 1).

the C-terminal truncated DDX3X construct is able to hydrolyze other nucleotides in addition to ATP and dATP. We used the malachite green/molybdate colorimetric assay[22] to investigate the ability of the C-terminal truncated DDX3X to hydrolyze all four nucleotides and deoxynucleotides in the presence or absence of substrate B:B. Our data show that different from the wild-type DDX3X, the C-terminal truncated DDX3X is able to hydrolyze cytidine triphosphate (CTP) both in the presence and absence of an RNA substrate and ATP and dATP only in the presence of RNA (Figure 3). Hence, the C-terminal truncated DDX3X construct is a more stringent NTPase and dNTPase than the wild-type protein.[20]

**During its ATP Hydrolysis Catalytic Cycle, the C-Terminal Truncated DDX3X Acts as a Multimer.** Finally, we investigated if the stimulation of ATP hydrolysis by substrate B:B was a cooperative process. Thus, we investigated, via thin-layer chromatography (TLC), the fraction of ATP hydrolyzed versus C-terminal truncated DDX3X concentration. As the data in Figure 4 show, the dependence of the ATP hydrolyzed on the protein concentration has a sigmoid shape, suggesting allosteric interactions. Hence, the Hill equation, instead of the Michaelis−Menten equation, was used to fit the data. The Hill constant obtained from this data is 1.99 ± 0.19, indicating that during its catalytic cycle the C-terminal truncated DDX3X acts as a multimer. This result is similar to the one obtained recently with a DDX3X construct containing residues 132−607.[38] Thus, the above construct has a truncated N-terminal domain but has 29 more C-terminal residues than the DDX3X construct used in this study. Finally, the wild-type DDX3X was shown to act as a multimer during its helicase catalytic cycle.[39]

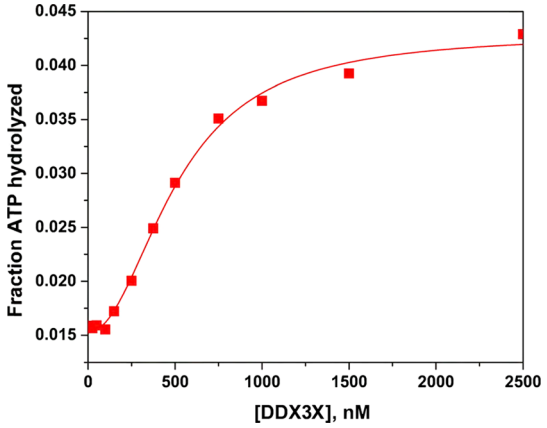


**Figure 4.** Dependence of the ATPase activity of DDX3X on protein concentration. The substrate used for this experiment is B (—square—), which contains single-stranded and double-stranded regions. The plot is representative of a single experiment. The Hill equation was used to fit the data. The Hill coefficient and dissociation constant average values and standard deviations, obtained from two independent experiments, are 1.99 ± 0.19 and 551 ± 50 nM, respectively.

## DISCUSSION

The C-terminal truncated DDX3X studied here behaved similarly to the wild-type LAF-1 protein.[17] Both the C-terminal truncated DDX3X and LAF-1 bind as multimeric protomer single-stranded RNA substrates and substrates containing single-stranded and double-stranded junctions (Figure 2). The fact that the C-terminal truncated DDX3X binds the RNA substrates as a multimer and acts, during the ATPase hydrolysis, as a multimer demonstrates that the lack of 80 residues from the C-terminal does not prevent DDX3X multimer formation (Figures 2 and 4).

Our results are in complete agreement with Ded1p, the DDX3X ortholog in *S. cerevisiae*.[40] Ded1p, which completely lacks the C-terminal domain, forms at a minimum a dimer.[40] Moreover, a DDX3X construct, which lacked most of the DDX3X N-terminal domain and 51 residues from its C-terminal domain, also formed a multimer.[38] Our results, combined with previous data, suggest that the minimally active DDX3X construct is sufficient for multimer formation. The majority of DDX3X N- and C-terminal residues are not required to form a DDX3X multimer.

Neither LAF-1 nor the C-terminal truncated DDX3X binds to blunt-ended double helices. On the other hand, the minimally active DDX3X construct was shown to bind to a blunt-ended double-helix RNA, though this helix did not


https://doi.org/10.1021/acsomega.1c00700
ACS Omega 2021, 6, 12640−12646

support its ATPase activity. Combined, our results and the previous data indicate that residues 1−131 of the N-terminal dictate the DDX3X protein's RNA substrate choice. An attractive hypothesis is that residues 1−131 of DDX3X have evolved to prevent DDX3X from binding to blunt-ended double helices.

The precise in vivo RNA substrates of DDX3X, like those of many DEAD-box proteins, remain largely uncharacterized.[3] Furthermore, DDX3X performs many of its cellular functions in concert with other proteins, which makes the characterization of DDX3X in vivo RNA substrates exceedingly difficult.[41] The experiments performed here also suggest that the DDX3X in vivo RNA substrates likely contain single-stranded RNA regions.

The dissociation constant of C-terminal truncated DDX3X binding to RNA substrate B:B as measured by the TLC ATPase assay is 551 ± 50 nM, while the dissociation constant as measured by EMSA is 285 ± 18 nM (Table 2 and Figure 4). These differences could imply that the DDX3X binding constant, as measured from the ATPase assay, contains contributions from other kinetic steps. Differences between the RNA binding affinity as measured via a direct assay such as EMSA and measured indirectly by an ATPase assay have been observed for other members of DEAD-box family of enzymes.[42]

Finally, the C-terminal truncated DDX3X, in addition to hydrolyzing ATP and dATP in the presence of an RNA substrate, hydrolyzes CTP both in the presence and absence of RNA. On the other hand, the wild-type DDX3X hydrolyzes all four NTPs and dNTPs in the presence and absence of the RNA substrates, while only ATP and dATP promote its helicase activity.[20,21,39] Future structural and biochemical experiments could shed light on the physiological importance of DDX3X hydrolyzing all four nucleotides and deoxynucleotides while using only ATP and dATP for its unwinding activity and on how the C-terminal of DDX3X modulates the DDX3X nucleotide specificity.

## METHODS

**Materials.** All chemicals were bought from Thermo Fisher Scientific. RNA substrates were commercially obtained and HPLC-purified from Integrated DNA Technologies. $\gamma$-$^{32}$P-labeled ATP was obtained from PerkinElmer. PEI cellulose F coated TLC plates were bought from EMD Millipore.

**Protein Expression and Purification.** The pNIC28 vector bearing the complete sequence of the wild-type DDX3X protein and an N-terminal His-tag with a TEV cleavage site (Supporting Information, Figure S1) was a gift from Dr. Helena Berglund at the Karolinska Institute. The wild-type DDX3X contains 662 amino acids and consists of the N-terminal domain, catalytic core, and C-terminal domain (Supporting Information, Figure S1). We substituted the sequence of amino acid 583 in the DDX3X coding sequence with that of a stop codon. Hence, our DDX3X construct lacks 80 C-terminal residues. Protein expression and purification were carried out as specified by Högbom et al.[13] In brief, the DDX3X construct bearing an N-terminal His-tag was expressed in *Escherichia coli* C2566I (NEB). Nickel affinity column (HisPur Ni-NTA Superflow Agarose, Thermo Scientific) and size-exclusion column (Sephacryl S-200HR, GE Healthcare Lifesciences) were used to purify the protein. The His-tag was not removed from DDX3X. The protein was stored at −80 °C in small aliquots, which were thawed only once before use and were never refrozen.

**Malachite Green ATPase Assay.** The malachite green/molybdate colorimetric assay was used to determine phosphate release.[22] The malachite green/molybdate solution consisted of 0.034% malachite green, 1.04% ammonium molybdate, and 1 M HCl. The RNA substrates were annealed by incubating them with 50 mM 4-(2-hydroxyethyl)-1-piperazineethanesulfonic acid (HEPES)-KOH pH 7.5, 50 mM KCl at 95 °C for 1 min, 65 °C for 3 min, cooling it down to 25 °C for 1 min, and adding 10 mM $MgCl_2$ final. The nucleotide hydrolysis reaction mixture consists of 1.5 $\mu$M annealed RNA, 50 mM HEPES-KOH, pH 7.5, 1.3 mM $MgCl_2$, 50 mM KCl, 1 mM dithiothreitol (DTT), 0.1 mg/mL BSA, and 1 $\mu$M DDX3X protein. The reaction was started by the addition of 0.5 mM NTP or dNTP final. The DDX3X nucleotide hydrolysis reaction was allowed to proceed at 37 °C for 30 min. Next, an equivalent volume of the DDX3X hydrolysis reaction and malachite green/molybdate solution was mixed and incubated at 22 °C for 5 min. After 5 min, the absorbance of solution at 640 nm was measured.

**RNA Binding Gel-Shift Assay.** EMSA has been used extensively and successfully to measure the affinities for RNA substrates of DEAD-box proteins in general, DDX3X orthologs in other organisms, and a DDX3X construct for RNA in the presence and/or absence of AMPPNP.[12,14,17,29,30,37,43−46] For these experiments, RNA substrates were annealed as described for the malachite green assay. Final annealed RNA (1 nM) was incubated with different concentrations of DDX3X in 50 mM HEPES-KOH pH 7.5, 50 mM KCl, 1.3 mM $MgCl_2$, 2 mM DTT, and 20% glycerol in the presence or absence of 6 mM final AMPPNP·Mg. The reaction mixture was incubated for 30 min at 22 °C and then loaded on a nondenaturing gel. The nondenaturing gel was 10% polyacrylamide with a ratio of acrylamide/bis-acrylamide of 29:1. The gel buffer and the running buffer consisted of 0.33× TBE buffer and 5 mM $MgCl_2$. The gels were run at 22 °C for 2 h at a voltage of 10 V·cm$^{-1}$. Next, the gels were dried in a Gel Dryer (Model 583, Bio-Rad Laboratories) and exposed to a phosphor-imaging screen. Exposures were imaged using a Personal Molecular Imager System (Bio-Rad Laboratories) and analyzed using Quantity One (Bio-Rad Laboratories). The Hill equation was used to fit the data

$$f_B = f_B(0) + [f_B(\max) - f_B(0)]\left\{\frac{[\text{protein}]^n}{K_d{}^n + [\text{protein}]^n}\right\} \quad (1)$$

Here, (eq 1) $f_B$ is the fraction of RNA bound to protein. $f_B(0)$ and $f_B(\max)$ are the lower and upper baselines of the binding curve. $K_d$ is the dissociation constant and $n$ is the Hill coefficient. The program used to fit the data was OriginLab. All of the variables were allowed to float in OriginLab. The $K_d$ and the Hill coefficient values were determined using OriginLab. The average values and standard deviations for $K_d$ and Hill coefficient are shown in Table 2. The data shown in Figure 2 are raw unnormalized data.

**TLC ATPase Assay.** Hydrolysis of ATP was monitored using TLC, as previously described;[47] however, $\gamma$-$^{32}$P-labeled ATP was used instead of $\alpha$-$^{32}$P-labeled ATP. The TLC assay too has been used extensively to measure the ATP hydrolysis of DDX3X and other DEAD-box proteins.[39,47,48] The RNA was annealed similar to the malachite green assay.


https://doi.org/10.1021/acsomega.1c00700
ACS Omega 2021, 6, 12640−12646

Subsequently, different protein concentrations were mixed with 50 mM HEPES-KOH pH 7.5, 1.3 mM $MgCl_2$, 50 mM KCl, 2 mM DTT, 1 nM RNA, 2 mM ATP, and 0.01 $\mu$M $\gamma$-$^{32}$P-labeled ATP and incubated at 37 °C for 30 min. After incubation, the reactions were quenched with 0.5 M ethylenediaminetetraacetic acid (EDTA), pH 8, and spotted on PEI cellulose F coated TLC plates. The TLC plates were developed using a solvent system consisting of 0.75 M LiCl and 1 M acetic acid. TLC plates were left to dry then exposed to phosphor-imaging screens. The screens were scanned using a Personal Molecular Imager System (Bio-Rad Laboratories) and analyzed using Quantity One (Bio-Rad Laboratories). The fraction of ATP hydrolyzed was calculated as the ratio of the counts on the inorganic phosphate band over the total counts on the lane.

The Michaelis−Menten model cannot accurately describe the enzyme−ligand interaction when the allosteric interaction is observed and the Hill equation is often used. The Hill equation has also been used to determine the Ded1p, the DDX3X ortholog in *S. cerevisiae* helicase activity, wild-type DDX3X helicase activity, and N- and C-terminal truncated DDX3X ATPase activity.[38−40] The fractions of ATP hydrolyzed versus protein concentrations were fit in this study to eq 1 using OriginLab.

## ■ ASSOCIATED CONTENT

### Supporting Information

The Supporting Information is available free of charge at https://pubs.acs.org/doi/10.1021/acsomega.1c00700.

Amino acid sequence of the DDX3X construct used in this study (Figure S1); EMSA sample gels (Figure S2) (PDF)

## ■ AUTHOR INFORMATION


### Corresponding Author

**Eda Koculi** − *Department of Biology, Johns Hopkins University, Baltimore, Maryland 21218, United States;* orcid.org/0000-0001-9477-555X; Phone: 410-516-7314; Email: ekoculi1@jhu.edu; Fax: 410-516-5213

### Authors

†**Anthony F. T. Moore** − *Department of Chemistry, University of Central Florida, Orlando, Florida 32816, United States*

**Aliana López de Victoria** − *Department of Chemistry, University of Central Florida, Orlando, Florida 32816, United States*

Complete contact information is available at: https://pubs.acs.org/10.1021/acsomega.1c00700


### Notes

The authors declare no competing financial interest.

†Anthony F.T. Moore has passed away.

## ■ ACKNOWLEDGMENTS

This work was supported in part by the National Institute of Cancer (5R21CA175625 to E.K.) and the National Institute of General Medical Sciences (R01-GM131062 to E.K.).

## ■ REFERENCES


(1) Tanner, N. K.; Linder, P. DExD/H box RNA helicases: from generic motors to specific dissociation functions. *Mol. Cell* **2001**, *8*, 251−262.

(2) Linder, P.; Fuller-Pace, F. Happy birthday: 25 years of DEAD-box proteins. *Methods Mol. Biol.* **2015**, *1259*, 17−33.

(3) Linder, P.; Jankowsky, E. From unwinding to clamping - the DEAD box RNA helicase family. *Nat. Rev. Mol. Cell Biol.* **2011**, *12*, 505−516.

(4) Cordin, O.; Banroques, J.; Tanner, N. K.; Linder, P. The DEAD-box protein family of RNA helicases. *Gene* **2006**, *367*, 17−37.

(5) He, Y.; Zhang, D.; Yang, Y.; Wang, X.; Zhao, X.; Zhang, P.; Zhu, H.; Xu, N.; Liang, S. A double-edged function of DDX3, as an oncogene or tumor suppressor, in cancer progression (Review). *Oncol. Rep.* **2018**, *39*, 883−892.

(6) Kukhanova, M. K.; Karpenko, I. L.; Ivanov, A. V. DEAD-box RNA Helicase DDX3: Functional Properties and Development of DDX3 Inhibitors as Antiviral and Anticancer Drugs. *Molecules* **2020**, *25*, No. 1015.

(7) Juraschka, K.; Taylor, M. D. Medulloblastoma in the age of molecular subgroups: a review. *J. Neurosurg.* **2019**, *24*, 353−363.

(8) Riva, V.; Maga, G. From the magic bullet to the magic target: exploiting the diverse roles of DDX3X in viral infections and tumorigenesis. *Future Med. Chem.* **2019**, *11*, 1357−1381.

(9) Jarmoskaite, I.; Russell, R. RNA helicase proteins as chaperones and remodelers. *Annu. Rev. Biochem.* **2014**, *83*, 697−725.

(10) Thirumalai, D.; Lorimer, G. H.; Hyeon, C. Iterative annealing mechanism explains the functions of the GroEL and RNA chaperones. *Protein Sci.* **2020**, *29*, 360−377.

(11) López de Victoria, A.; Moore, A. F. T.; Gittis, A. G.; Koculi, E. Kinetics and Thermodynamics of DbpA Protein's C-Terminal Domain Interaction with RNA. *ACS Omega* **2017**, *2*, 8033−8038.

(12) Moore, A. F.; Gentry, R. C.; Koculi, E. DbpA is a region-specific RNA helicase. *Biopolymers* **2017**, *107*, No. e23001.

(13) Högbom, M.; Collins, R.; van den Berg, S.; Jenvert, R. M.; Karlberg, T.; Kotenyova, T.; Flores, A.; Karlsson Hedestam, G. B.; Schiavone, L. H. Crystal structure of conserved domains 1 and 2 of the human DEAD-box helicase DDX3X in complex with the mononucleotide AMP. *J. Mol. Biol.* **2007**, *372*, 150−159.

(14) Epling, L. B.; Grace, C. R.; Lowe, B. R.; Partridge, J. F.; Enemark, E. J. Cancer-associated mutants of RNA helicase DDX3X are defective in RNA-stimulated ATP hydrolysis. *J. Mol. Biol.* **2015**, *427*, 1779−1796.

(15) Floor, S. N.; Condon, K. J.; Sharma, D.; Jankowsky, E.; Doudna, J. A. Autoinhibitory Interdomain Interactions and Subfamily-specific Extensions Redefine the Catalytic Core of the Human DEAD-box Protein DDX3. *J. Biol. Chem.* **2016**, *291*, 2412−2421.

(16) Henn, A.; Bradley, M. J.; De La Cruz, E. M. ATP utilization and RNA conformational rearrangement by DEAD-box proteins. *Annu. Rev. Biophys.* **2012**, *41*, 247−267.

(17) Kim, Y.; Myong, S. RNA Remodeling Activity of DEAD Box Proteins Tuned by Protein Concentration, RNA Length, and ATP. *Mol Cell* **2016**, *63*, 865−876.

(18) Putnam, A. A.; Jankowsky, E. DEAD-box helicases as integrators of RNA, nucleotide and protein binding. *Biochim. Biophys. Acta, Gene Regul. Mech.* **2013**, *1829*, 884−893.

(19) Mallam, A. L.; Sidote, D. J.; Lambowitz, A. M. Molecular insights into RNA and DNA helicase evolution from the determinants of specificity for a DEAD-box RNA helicase. *eLife* **2014**, *3*, No. e04630.

(20) You, L. R.; Chen, C. M.; Yeh, T. S.; Tsai, T. Y.; Mai, R. T.; Lin, C. H.; Lee, Y. H. Hepatitis C virus core protein interacts with cellular putative RNA helicase. *J. Virol.* **1999**, *73*, 2841−2853.

(21) Franca, R.; Belfiore, A.; Spadari, S.; Maga, G. Human DEAD-box ATPase DDX3 shows a relaxed nucleoside substrate specificity. *Proteins* **2007**, *67*, 1128−1137.

(22) Cho, H. J.; Ramer, S. E.; Itoh, M.; Winkler, D. G.; Kitas, E.; Bannwarth, W.; Burn, P.; Saito, H.; Walsh, C. T. Purification and characterization of a soluble catalytic fragment of the human transmembrane leukocyte antigen related (LAR) protein tyrosine phosphatase from an *Escherichia coli* expression system. *Biochemistry* **1991**, *30*, 6210−6216.

(23) Weiss, J. N. The Hill equation revisited: uses and misuses. *FASEB J.* **1997**, *11*, 835−841.
(24) Zuker, M. Mfold web server for nucleic acid folding and hybridization prediction. *Nucleic Acids Res.* **2003**, *31*, 3406−3415.
(25) Hellman, L. M.; Fried, M. G. Electrophoretic mobility shift assay (EMSA) for detecting protein-nucleic acid interactions. *Nat. Protoc.* **2007**, *2*, 1849−1861.
(26) Woodson, S. A.; Koculi, E. Analysis of RNA folding by native polyacrylamide gel electrophoresis. *Methods Enzymol.* **2009**, *469*, 189−208.
(27) Karginov, F. V.; Uhlenbeck, O. C. Interaction of *Escherichia coli* DbpA with 23S rRNA in different functional states of the enzyme. *Nucleic Acids Res.* **2004**, *32*, 3028−3032.
(28) Sengoku, T.; Nureki, O.; Nakamura, A.; Kobayashi, S.; Yokoyama, S. Structural basis for RNA unwinding by the DEAD-box protein Drosophila Vasa. *Cell* **2006**, *125*, 287−300.
(29) Elles, L. M.; Uhlenbeck, O. C. Mutation of the arginine finger in the active site of *Escherichia coli* DbpA abolishes ATPase and helicase activity and confers a dominant slow growth phenotype. *Nucleic Acids Res.* **2008**, *36*, 41−50.
(30) Karginov, F. V.; Caruthers, J. M.; Hu, Y.; McKay, D. B.; Uhlenbeck, O. C. YxiN is a modular protein combining a DEx(D/H) core and a specific RNA-binding domain. *J. Biol. Chem.* **2005**, *280*, 35499−35505.
(31) Del Campo, M.; Lambowitz, A. M. Structure of the Yeast DEAD box protein Mss116p reveals two wedges that crimp RNA. *Mol. Cell* **2009**, *35*, 598−609.
(32) Bono, F.; Ebert, J.; Lorentzen, E.; Conti, E. The crystal structure of the exon junction complex reveals how it maintains a stable grip on mRNA. *Cell* **2006**, *126*, 713−725.
(33) von Moeller, H.; Basquin, C.; Conti, E. The mRNA export protein DBP5 binds RNA and the cytoplasmic nucleoporin NUP214 in a mutually exclusive manner. *Nat. Struct. Mol. Biol.* **2009**, *16*, 247−254.
(34) Andersen, C. B.; Ballut, L.; Johansen, J. S.; Chamieh, H.; Nielsen, K. H.; Oliveira, C. L.; Pedersen, J. S.; Seraphin, B.; Le Hir, H.; Andersen, G. R. Structure of the exon junction core complex with a trapped DEAD-box ATPase bound to RNA. *Science* **2006**, *313*, 1968−1972.
(35) Collins, R.; Karlberg, T.; Lehtio, L.; Schutz, P.; van den Berg, S.; Dahlgren, L. G.; Hammarstrom, M.; Weigelt, J.; Schuler, H. The DEXD/H-box RNA helicase DDX19 is regulated by an {alpha}-helical switch. *J. Biol. Chem.* **2009**, *284*, 10296−10300.
(36) Aregger, R.; Klostermeier, D. The DEAD box helicase YxiN maintains a closed conformation during ATP hydrolysis. *Biochemistry* **2009**, *48*, 10679−10681.
(37) Iost, I.; Dreyfus, M.; Linder, P. Ded1p, a DEAD-box protein required for translation initiation in *Saccharomyces cerevisiae*, is an RNA helicase. *J. Biol. Chem.* **1999**, *274*, 17677−17683.
(38) Song, H.; Ji, X. The mechanism of RNA duplex recognition and unwinding by DEAD-box helicase DDX3X. *Nat. Commun.* **2019**, *10*, No. 3085.
(39) Sharma, D.; Putnam, A. A.; Jankowsky, E. Biochemical Differences and Similarities between the DEAD-Box Helicase Orthologs DDX3X and Ded1p. *J. Mol. Biol.* **2017**, *429*, 3730−3742.
(40) Putnam, A. A.; Gao, Z.; Liu, F.; Jia, H.; Yang, Q.; Jankowsky, E. Division of Labor in an Oligomer of the DEAD-Box RNA Helicase Ded1p. *Mol. Cell* **2015**, *59*, 541−552.
(41) Mo, J.; Liang, H.; Su, C.; Li, P.; Chen, J.; Zhang, B. DDX3X: structure, physiologic functions and cancer. *Mol. Cancer* **2021**, *20*, No. 38.
(42) Tsu, C. A.; Kossen, K.; Uhlenbeck, O. C. The *Escherichia coli* DEAD protein DbpA recognizes a small RNA hairpin in 23S rRNA. *RNA* **2001**, *7*, 702−709.
(43) Hardin, J. W.; Hu, Y. X.; McKay, D. B. Structure of the RNA binding domain of a DEAD-box helicase bound to its ribosomal RNA target reveals a novel mode of recognition by an RNA recognition motif. *J. Mol. Biol.* **2010**, *402*, 412−427.
(44) Polach, K. J.; Uhlenbeck, O. C. Cooperative binding of ATP and RNA substrates to the DEAD/H protein DbpA. *Biochemistry* **2002**, *41*, 3693−3702.
(45) Khoshnevis, S.; Askenasy, I.; Johnson, M. C.; Dattolo, M. D.; Young-Erdos, C. L.; Stroupe, M. E.; Karbstein, K. The DEAD-box Protein Rok1 Orchestrates 40S and 60S Ribosome Assembly by Promoting the Release of Rrp5 from Pre-40S Ribosomes to Allow for 60S Maturation. *PLoS Biol.* **2016**, *14*, No. e1002480.
(46) Banroques, J.; Doere, M.; Dreyfus, M.; Linder, P.; Tanner, N. K. Motif III in superfamily 2 "helicases" helps convert the binding energy of ATP into a high-affinity RNA binding site in the yeast DEAD-box protein Ded1. *J. Mol. Biol.* **2010**, *396*, 949−966.
(47) Garcia, I.; Albring, M. J.; Uhlenbeck, O. C. Duplex destabilization by four ribosomal DEAD-box proteins. *Biochemistry* **2012**, *51*, 10109−10118.
(48) Gentry, R. C.; Childs, J. J.; Gevorkyan, J.; Gerasimova, Y. V.; Koculi, E. Time course of large ribosomal subunit assembly in *E. coli* cells overexpressing a helicase inactive DbpA protein. *RNA* **2016**, *22*, 1055−1064.


https://doi.org/10.1021/acsomega.1c00700
*ACS Omega* 2021, 6, 12640−12646